Formation and electronic states of In nanoclusters on the Si(111)-7×7 surface

Jung Hoon Byun, Jin Sung Shin, Pil Gyu Kang, Hojin Jeong, and Han Woong Yeom*
Institute of Physics and Applied Physics and Center for Atomic Wires and Layers, Yonsei University, Seoul 120-746, Republic of Korea
(Received 17 March 2009; published 16 June 2009)

The formation and evolution of submonolayer In clusters on the Si(111)-7×7 surface at different temperatures were investigated using scanning tunneling microscopy. The electronic states of the well-defined nanoclusters were studied by scanning tunneling spectroscopy (STS). The well-ordered triangular In "magic" clusters are formed at ~200 °C within 7×7 half-unit cells as reported previously. The STS measurement reveals the semiconducting property of In magic clusters with a substantial energy gap of 0.8 eV in accordance with the recent photoemission study. The band gap is very asymmetric with a shallow unoccupied state due to the pseudomolecular orbitals of the In-Si bond network, as revealed by the density-functional calculation for the existing structure model with six In atoms. The electronic modification of Si adatoms in the neighboring sites was observed. At a lower temperature than that of the magic cluster formation, we observed a different type of nanoclusters formed in faulted half-unit cells with an identical size. This cluster has a characteristic asymmetric shape with chirality. These nanoclusters are thought to consist of a similar number of In atoms and are the precursory state to the magic cluster formation. The STS result for the initial cluster shows a distinct semiconducting property with a significantly reduced band gap of 0.4 eV.

DOI: 10.1103/PhysRevB.79.235319 PACS number(s): 68.37.Ef, 68.43.Hn, 73.20.At

I. INTRODUCTION

The initial growth of indium on the Si(111)-7×7 surface has been investigated extensively. It shows active surface phase transformations depending on the In coverage and the substrate temperature with a rich series of well-ordered phases such as $\sqrt{3}\times\sqrt{3}$, $\sqrt{31}\times\sqrt{31}$, 4×1, $\sqrt{7}\times\sqrt{3}$, and 2×2.[1–4] These surface structures show diverse and interesting electronic properties. The $\sqrt{3}\times\sqrt{3}$ surface is semiconducting, while the 4×1 and $\sqrt{7}\times\sqrt{3}$ surfaces have strong one- and two-dimensional metallic property, respectively.[5–7] These systems traditionally provided model systems to study fundamental aspects of the metal/semiconductor interface formation and, recently, new playgrounds for the investigation of low dimensional metals. More recently, these surface phases have also been used as templates to build up ordered nanostructure arrays.[8–10]

On the other hand, at lower In coverages and lower temperature than the above surface phases, the formation of a well-ordered nanoclusters array was reported recently.[11,12] The clusters form within each half-unit cells (HUCs) of the Si(111)-7×7 surface with an identical size and shape, which are, thus called "magic clusters." The widely accepted structure model for the magic cluster consists of six In atoms and three displaced Si adatoms forming a triangular in-plane cluster.[11,13] Similar nanocluster formation was also reported for other group-III metals as well as various other metal adsorbates such as Na, Pb, and Ag with varying structures.[13–19] While previous studies on the magic clusters have focused on the growth and atomic structures, the formation mechanism, electronic states, and other physical properties of the clusters are largely unknown. As for the electronic states, our recent photoemission study showed the semiconducting property of In magic clusters.[20] A recent scanning tunneling spectroscopy (STS) study has reported consistent semiconducting nature of the Al magic cluster and measured the band gap quantitatively as 1.7 eV. However, this band gap is much larger than that predicted by the density-functional theory and the discrepancy was attributed to the tip-induced band bending.[21] On the other hand, our previous study also found that at lower temperatures than the magic cluster formation, In adsorbates form a distinct type of clusters, called initial clusters, which transform into magic clusters by postannealing.[20] The detailed structural and electronic properties of these initial clusters are veiled, which may be important to understand the formation mechanism of the magic cluster.

In this paper, we investigated the atomic and electronic structure evolutions of In clusters on the Si(111)-7×7 surface at various temperatures. We reproduced the In magic clusters at ~200 °C and their electronic states were detailed by STS for different sites within a cluster and neighboring bare Si atoms. The STS result shows the semiconducting electronic property of the In magic cluster with a band gap of 0.8 eV, which is consistent with the previous photoemission study.[20,22] The interaction of the neighboring Si adatoms with the magic cluster was indicated. Our first-principles calculation reproduces the experimental results reasonably and explains the origin of the band gap as the bonding-antibonding type energy gap for the pseudomolecular orbitals of the In-Si bond network. The detailed structure of the initial cluster, formed at room temperature (RT), was revealed. The initial In clusters have an identical size and consistent shapes; asymmetric, chiral shapes with two different chiralities and three different orientations. The STS measurement of the initial cluster shows nonmetallic property with a significantly reduced band gap of 0.4 eV compared to the magic cluster. While the detailed atomic structure of the initial cluster is uncertain, it is thought to be a precursor state for the magic cluster formation.

II. EXPERIMENTAL DETAILS

Scanning tunneling microscopy (STM) measurements were carried out with a commercial variable-temperature

STM (Omicron, Germany) at RT under the base pressure below 1×10^{-11} torr. Chemically etched, *in situ*-heated and -sputtered W tips were employed. A mirror-polished *n*-type Si(111) sample (P doped, 2–8 Ω cm) was degassed rigorously at 600 °C. The clean Si(111)-7×7 surface was prepared by annealing at 850 °C after flash heating at 1230 °C by direct current flow. Indium was thermally evaporated from a well-outgassed graphite effusion cell. During the evaporation, the pressure was kept below 1.0×10^{-10} torr. Each point STS spectrum (dI/dV) was taken by averaging about 10 spectra from equivalent sites. First-principles total-energy calculations were performed using the Vienna *ab initio* simulation package[23] with ultrasoft pseudopotentials[24] and generalized-gradient approximation[25] in order to explore the local density of states (LDOS). The Si(111)7×7 surface was modeled by a repeated slab with six Si layers and a H layer terminating the bottommost Si layer. In 4*d* electrons were not included into the pseudopotentials but treated as valence electrons for a higher accuracy. The simulated STM images were obtained by integrating the LDOS from a given bias voltage to the Fermi energy.

III. RESULTS AND DISCUSSION

A. Electronic structure of magic cluster

Figure 1 shows the Si(111)-7×7 surfaces after In adsorption at 200 °C. This temperature was reported as the optimum temperature to form the ordered magic cluster array.[11] The detailed temperature dependence of the cluster formation was also surveyed in our previous photoemission study, which found the magic cluster formation at the range of 150~280 °C.[20] The triangular protrusions in Fig. 1(a) are such magic clusters reported previously. There exists a strong preference of the faulted HUCs over the unfaulted ones in the cluster formation.[12] Until the occupation of all faulted HUCs at 0.12 ML, the STM images [Fig. 1(a)] shows that 92% of the clusters are formed on faulted HUCs in average. This preference yields a very well-ordered array near 0.12 ML with uniquely oriented clusters. As increasing the In coverage over 0.12 ML, unfaulted HUCs are also occupied and saturated at 0.24 ML. At this coverage, another well-ordered cluster array is formed as shown in Fig. 1(b) but with two different cluster orientations. This array has a honeycomb pattern and a good long-range order.

The high-resolution dual-bias STM images in Figs. 1(c) and 1(d) show the detailed topography of the magic cluster within the fully ordered array.[11,13] The STM images of the cluster exhibit a strong polarity dependence; six bright protrusions in a triangle appears along with weaker protrusions of three Si corner adatoms in the empty state while only three weak protrusions merged into a compact triangle are observed with corner adatoms of enhanced contrast in the filled state. According to the recent structure model, the six bright protrusions in the empty state correspond to the positions of In atoms and the three in the filled state coincide with the positions of displaced Si adatoms.[11,12] The strong triangular contrasts appear above +0.5 V in the empty state and below −1.0 V in the filled state, as detailed in Fig. 2, indicating that the corresponding electronic states of the

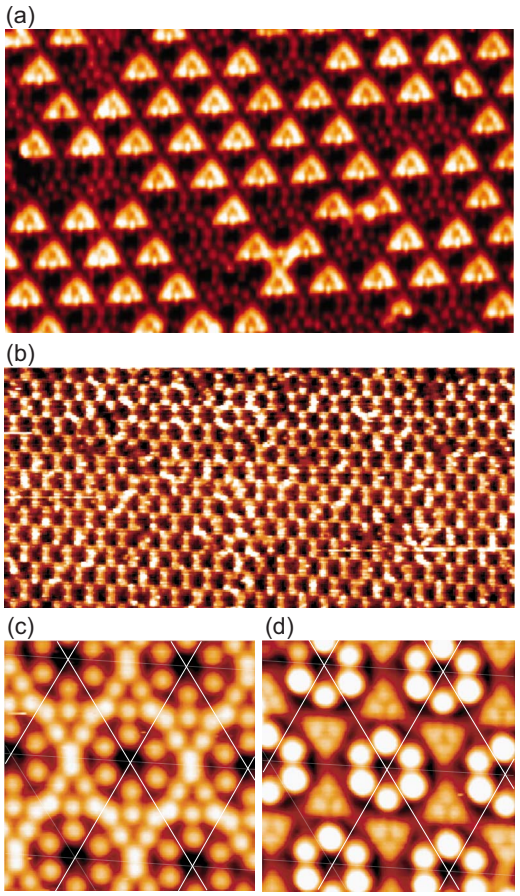

FIG. 1. (Color online) (a) STM topographic image of the Si(111)-7×7 surface after 0.1 ML of In deposition at 200 °C (27 nm×18 nm, V_s=+1.0 V). (b) The long-range ordered In magic cluster array at 0.24 ML (65 nm×30 nm, V_s=+1.8 V). Each bright protrusion in this figure corresponds to the individual In magic cluster. High-resolution STM images of the In magic clusters for the surface shown in (b) at (c) filled (−1.2 V) and (d) empty (+1.2 V) states. Guide lines in the figures enclose the 7×7 unit cells.

cluster are away from the Fermi energy. In contrast, in the sample bias near the Fermi energy, between −0.65 and +0.15 V, no clear feature can be seen for the cluster. It suggests the existence of an energy gap near the Fermi level. In Fig. 2, one can also notice that the Si corner adatoms of the

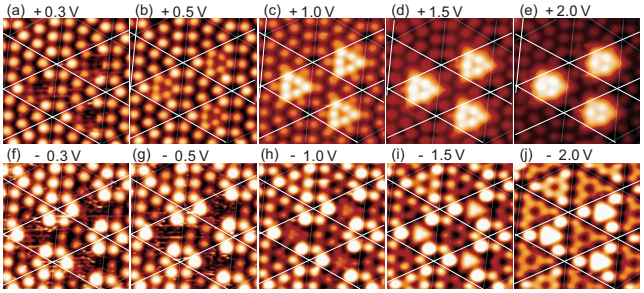

FIG. 2. (Color online) Bias-dependent (V_s=−2.0 V~+2.0 V) STM topographic images of the three adjacent In magic clusters formed at a very low coverage of about 0.05 ML. Guide lines in the figures enclose the 7×7 unit cells.

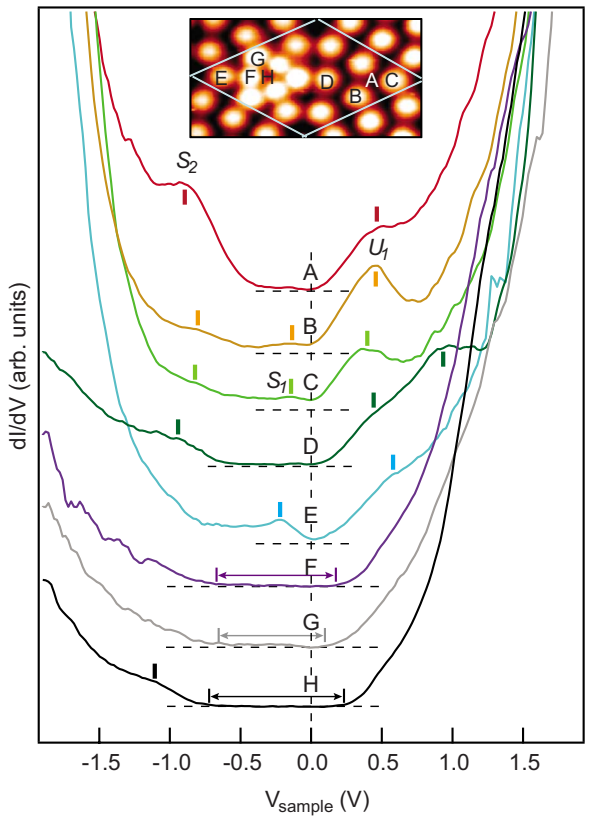

FIG. 3. (Color online) Site-resolved dI/dV spectra on the In magic clustered surface at RT. Capital alphabets in the inset images indicate the locations on which the spectra were acquired. Spectra were measured at a set condition of V_s=+1.0 V and I_t=0.05 nA.

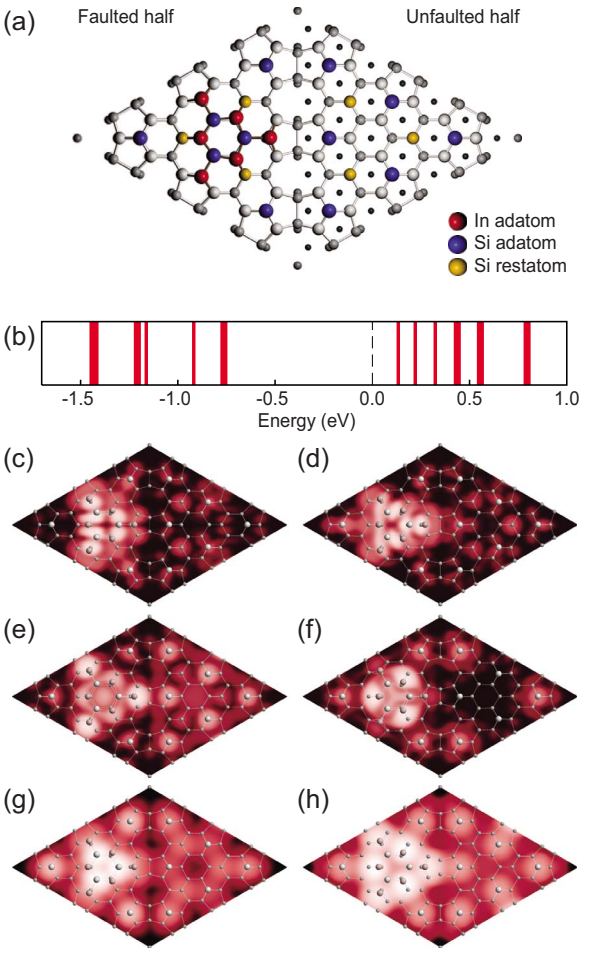

FIG. 4. (Color online) (a) Schematics of the atomic structure model for the In magic cluster on the Si(111)-7×7 unit cell. (b) Calculated energy spectrum of the electronic states for the In magic cluster where thicker bars represent doubly degenerated states. [(c) and (d)] LDOS map of doubly degenerated HOMO 1 and HOMO 2 electronic states at −0.75 eV. [(e) and (f)] LDOS map of LUMO 1 and LUMO 2 electronic states at 0.1 and 0.2 eV, respectively. [(g) and (h)] Simulated STM images (integrated LDOSs) of −1.5 and +0.8 V, respectively.

clustered HUC are brighter in filled states than those in bare 7×7 unit cells. Moreover, the Si center adatoms nearest the In magic clusters in the neighboring bare HUCs appear darker in the filled state than other adatoms. These observations indicate a complicated electronic interaction involving the Si adatoms not only within the clustered HUC but also within the neighboring HUC. A more detailed spectroscopic study is thus required to understand the STM image characteristics and the electronic states of the cluster and its neighbors.

The point STS dI/dV spectra measured for different sites within the clustered HUC and the neighboring bare HUC are shown in Fig. 3, which reveal the electronic state of the cluster and the electronic perturbation on its neighbors. In the neighboring HUC, the well-established surface states of Si adatoms (S_1 at ~−0.2 eV and U_1 at ~+0.4 eV on the sites B and C) and Si restatoms (S_2 at ~−0.9 eV on the site A) are clearly observed.[26,27] The spectra for the cluster are obtained on three inequivalent positions, that is, on the center of the cluster (the site H), on the apex of the empty-state triangle (the site G) and on the center of the triangle edge (the site F) as shown in the inset of the figure. However, all these spectra are more or less the same with null intensity near the Fermi level and weak spectral features at −1.1 and 0.5 eV. The null intensity clearly indicates the existence of the band gap which differs marginally from site to site: 0.9, 0.8, and 1.0 eV for the F, G, and H sites, respectively. It is interesting that the band gap is very asymmetric with its center located at 0.2~0.3 eV below the Fermi level. This result is consistent with the recent photoemission study, which found no density of states at least down to about −0.5 eV from the Fermi level.[20] Previous density-functional theory calculation has indicated that the density of states contribution from In does not exist within −1.5~1.0 eV.[22] This calculation, however, did not provide any detailed information for the In-Si (or In-In) bonding within the cluster.

In order to clarify the origin of the band gap and the spectral features of the cluster, we performed our own density-functional theory calculation based on pseudopotentials,[24] the generalized-gradient approximation,[25] and the slab geometry. We used the present structure model of the magic cluster as shown in Fig. 4(a) with six In atoms: three In atoms sit on the Si adatom positions making the apexes of the triangle and the displaced Si center adatoms form a hexagonal structure with the other three In atoms bonded to Si

restatoms. The triangles of six protrusions in the empty-state STM image thus correspond to the In atoms and the three Si adatoms displaced are located inside of that triangle. This In-Si bond network saturates all dangling bonds of the involved atoms: In atoms, Si restatoms, and Si center adatoms. The calculated energy spectra involving In valence electrons are displayed in Fig. 4(b) for experimentally relevant energy range. These energy levels correspond to the pseudomolecular orbitals of the magic cluster due to its In-Si bond network. For now, we can confirm the existence of the characteristically asymmetric band gap for the cluster. The band gap is centered at 0.3 eV below the Fermi level and its size is about 0.8 eV, which agree fairly well with the experiment.

The electron densities for the two highest occupied molecular orbitals (HOMO 1 and HOMO 2) and the two lowest unoccupied molecular orbitals (LUMO 1 and LUMO 2) are shown in Figs. 4(c)–4(f). From the symmetry of the electron density, it can be easily noticed that the HOMO and LUMO states basically correspond to the bonding and antibonding states of the In-Si bonds. In particular, the HOMO 1 and HOMO 2 states come mainly from the In-Si backbonds of the corner and center In atoms, respectively. When integrated over the given energy ranges, these energy levels reproduce well the characteristic STM images of the filled and empty states as shown in Figs. 4(g) and 4(h). Therefore, from these calculations one can understand that the microscopic origin of the band gap and the measured spectral features near the Fermi level is due to the pseudomolecular orbitals of the cluster which originate from the bonding and antibonding states of In-Si bonds. The good agreement between the theory and experiment also provides a further support to the present structure model for the magic cluster. This result is, however, not fully consistent with the previous density-functional theory calculation, which reported no In-induced states for the present energy range.[20,22] The reason for this discrepancy is not clear. The gap size of 0.8 eV is significantly smaller than that reported for the Al magic cluster of 1.7 eV.[21] The theoretical calculation for the Al cluster, however, yields a much smaller energy gap of 0.6 eV, which is similar to the present result.[22] While the authors of this work invoked the tip-induced band bending effect to explain this discrepancy, any sign of a significant tip effect has not been found. It can be due to the difference in the measurement conditions such as the tunneling current.

The influence on the electronic structure of the neighboring Si adatoms from the magic cluster is also observed by STS measurements in Fig. 3. While the spectra on the A, B, and C sites of the neighboring HUC exhibit no noticeable difference from those on the normal 7×7 HUC, that on the D site, the nearest Si adatom to the cluster, exhibits a fully depleted intensity for the S_1 dangling-bond state. This electronic change explains the reduced contrast on the D site in the filled-state topography mentioned above. The U_1 dangling-bond state is also reduced consistently and a new spectral feature develops at $\sim$0.9 V in the empty state. On the contrary, we find the enhanced intensity for S_1 on the unreacted Si corner adatoms in the clustered HUC (the site E). This is consistent with the enhanced contrast on this site in the filled-state STM images. Roughly speaking, the observed perturbations in the neighboring Si adatoms can be termed as a change of the electron filling in their dangling bonds (the S_1 state). It has been well known that the electron filling of the adatom dangling bonds is determined by the charge-transfer interaction with the neighboring Si restatom dangling bonds; electrons are transferred into the restatoms from the adatoms. Since the In clusters saturate the Si restatom dangling bonds by In-Si covalent bondings, the electron back donation from the restatoms into the neighboring Si adatoms is expected. Thus, it is highly likely that the increase of the S_1 state on the E site is due to such an electron back donation. The change in the D site in the neighboring unit cell could be more complicated and indirect with the possible effect of the strain induced by the cluster formation. Whatever the origin is, the perturbation in the neighboring unfaulted HUC by the cluster formation can, in turn, affect the cluster formation energy. This can partly contribute to the strong preference of the faulted HUC in the cluster formation.

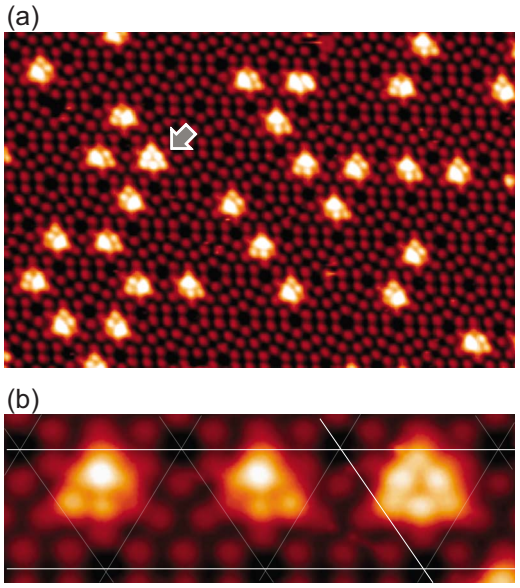

FIG. 5. (Color online) (a) STM topographic image (27×18 nm^2) of the Si(111)-7×7 surface after 0.05 ML of In deposition at RT (V_s=+1.8 V). (b) The magnified STM topographic image of the initial clusters with different chirality and the In magic cluster. Guide lines in the figure enclose the 7×7 unit cells.

B. Initial cluster at room temperature

Although the magic clusters are formed even at room temperature [see the arrow in Fig. 5(a)], their population is very low—below 5%. Instead, most of In adsorbates condense into a distinct form of clusters as shown in Fig. 5. Although the shape of these clusters, the initial clusters hereafter, looks rather irregular at a first glance, a closer look reveals that the clusters have very consistent shapes. Figure 5(b) shows more detailed image of three adjacent clusters, two initial clusters, and one magic cluster. The shape of the initial cluster is asymmetric with three protrusions at this empty-state bias: a very strong one and two weaker ones. Thus the threefold rotational symmetry of the magic cluster

is lost. Instead, due to the asymmetric location of the two weak protrusions, the initial cluster has the chiral symmetry with two chiral structures shown in the figure. There is no preference for one chiral form in the formation of these clusters with an equal population within the experimental error. The two chiral forms and the three rotational orientations due to the lack of the rotational symmetry provide an impression that the initial clusters are disordered. However, it is true that there exists a unique cluster structure and all the clusters are formed on the faulted HUC. As in the case of the magic cluster, the preference of the faulted HUC persists up to the depletion of all faulted HUC sites at 0.12 ML. By comparing the number of clusters formed for the same amount of deposited In, we find that the number of In atoms involved in a single initial cluster is the same as that of the magic cluster. This can also be directly confirmed by a postannealing experiment; an annealing above 200 °C converts all initial clusters into magic clusters of a similar number. That is, the initial cluster is metastable and highly likely a precursor structure in the formation of the magic cluster.

A distinct adsorption state below 150 °C down to −110 °C was identified by our recent photoemission study while its detailed structure was not clarified. The earlier STM study for the RT growth reported three types of cluster structures and their structure models were also proposed.[28] One of the types corresponds to the In magic cluster and another one seems to be the initial cluster observed here. The third type could not have been identified in the present work. The atomic structures for these clusters were explained basically with In adsorbates on the 7×7 structure without any significant displacement of Si atoms. Our theoretical study indicates that these simple structure models cannot yield energetically stable structures and cannot properly explain the STM images in contrast to the recent structure model of the magic cluster. The recent STM studies also noticed a different form of clusters during the magic cluster formation, which is actually consistent with the initial clusters.[12,19] One of these studies suggested the initial cluster as the magic cluster with an extra In atom on top of the apparent shape of the cluster. This idea cannot explain the fact that the initial clusters are formed at a lower temperature than the magic cluster and transform into the magic cluster by the thermal activation.

The STM image of the initial cluster exhibits a strong bias dependence, suggesting the complexity of its atomic structure. Figure 6 compares the detailed bias-dependent STM images of the initial cluster to those of the magic cluster formed nearby. At lowest biases of both filled and empty states [(d) and (h)], two of the three Si center adatoms disappear in the HUC with an initial cluster while all three center adatoms disappear for the magic cluster. The remaining adatom corresponds to the dark part (or the missing apex of a triangle) of the initial cluster in the empty-state image (1.5 V) of Fig. 5. This strongly suggests that one center adatom is not displaced by In in the initial cluster. The corresponding center adatom, however, appears stronger at the higher bias in the filled state. At a higher bias than 0.3 V in the empty state, one can notice the strong protrusion near, but not exactly on, one Si center adatom position, which was mentioned above for the high empty-state bias image of Fig. 5. At +1.0 V in the empty state, the initial cluster appears fairly symmetric and indeed looks like a magic cluster with an extra In atom on top. This structure is, however, not consistent with the images of other bias conditions. We have tried to construct an atomic structure model of the initial cluster based on these characteristic STM images. However, numerous candidate structures could not pass through the test of the energetical stability and the consistency of the simulated STM images through the density-functional theory calculations so far. Thus, the atomic structure of the initial cluster requires further studies, which would be important to understand the kinetic and energetic pathways to the magic cluster formation.

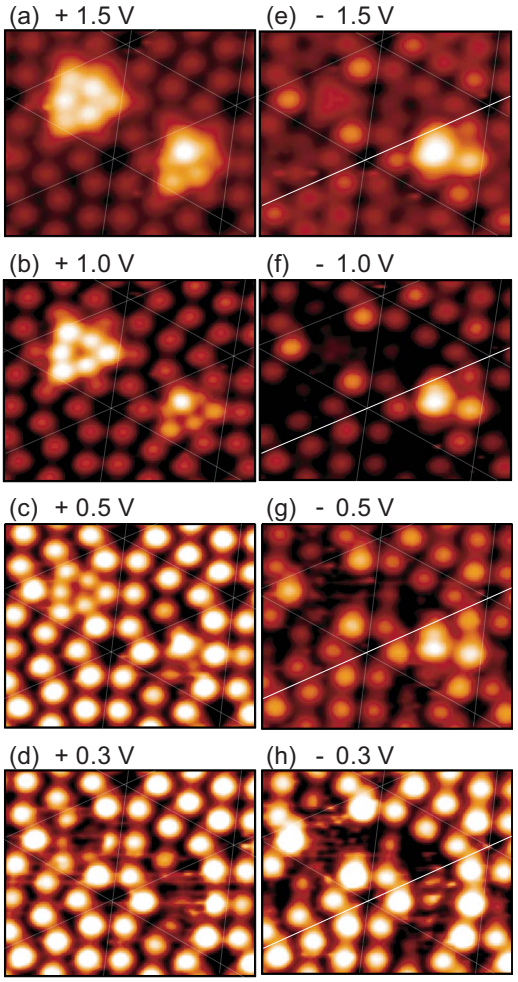

FIG. 6. (Color online) Bias-dependent (V_s=−1.5 V∼+1.5 V) STM topographic images of the initial cluster with the In magic cluster for comparing. Guide lines in the figures enclose the 7×7 unit cells.

The initial clusters possess a distinct electronic property. Figure 7 shows the point STS dI/dV spectra measured on different sites within the initial cluster and the neighboring Si sites. The overall spectral shapes for H and I sites of the initial cluster are rather similar to those on the same sites (i.e., on the In atoms) of the In magic cluster except for a much reduced band gap. A weak spectral feature exists around 0.6 eV in the filled state, which reduces the gap size to about 0.4 eV, about half of that for the magic cluster. The

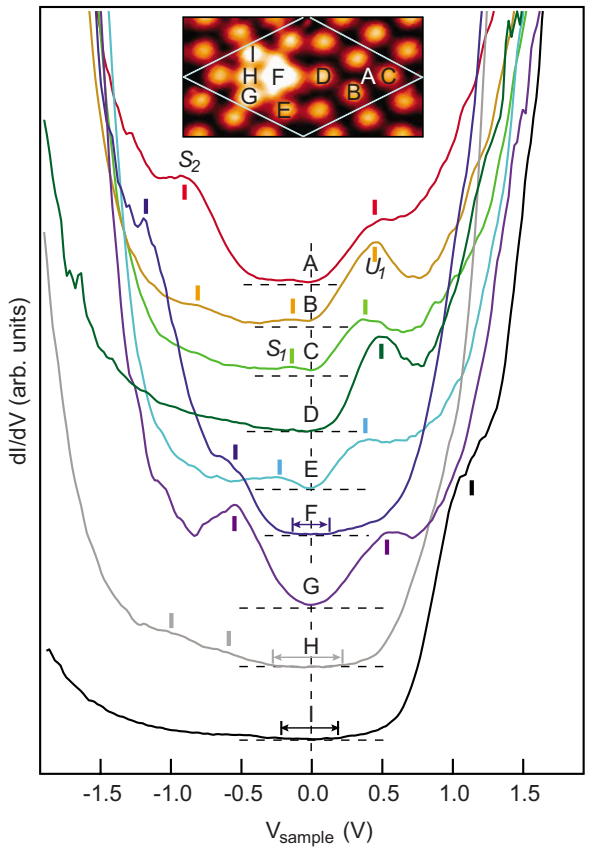

FIG. 7. (Color online) Site-resolved dI/dV spectra on the In initial clustered surface at RT. Capital alphabets in the inset images indicate the locations on which the spectra were acquired. The spectra were measured at a set condition of V_s=+1.0 V and I_t =0.05 nA.

reduced band gap seems consistent with the metastable nature of the initial cluster compared to the magic cluster since the large band gap would contribute to the stability of the cluster through the electronic energy gain. On the G site of the initial cluster, the state at −0.6 eV is prominent along with an unoccupied state at 0.6 eV. The site G corresponds to the undisplaced Si center adatom. Then, the state at 0.6 eV can be identified as the unoccupied dangling-bond state U_1 of the Si adatom. However, the strong state at −0.6 eV indicates that this adatom is strongly affected by the cluster formation. On the most prominent protrusion of the initial cluster, the site F, we find a smaller band gap of 0.3 eV with two spectral features at −0.6 and −1.1 eV. Our previous photoemission study observed a spectral feature at −0.6 eV at the temperature range for the magic cluster formation.[20] This rather weak spectral feature could be due to the filled state observed on the F and G sites of the initial clusters, which could be mixed with magic clusters. The influence in the electronic structure on the neighboring Si adatoms is also observed for the initial cluster formation. Basically, the influence of the initial cluster is not substantially different from that of the magic cluster. S_1 on the Si corner adatom of the same HUC (the site E) is enhanced while that on the nearest-neighbor Si adatom (the site D) of the next HUC is reduced. However, the development of new spectral features is not observed on the D site in contrast to the magic cluster case.

IV. SUMMARY

The formation and evolution of In clusters on the Si(111)-7×7 surface were investigated by STM at the substrate temperature from RT to 400 °C. In addition, the electronic structures of the well-defined clusters were studied by STS. As indium is evaporated onto the Si(111)-7×7 surface at the substrate temperature of 200 °C, the well-known triangular magic clusters dominate on the surface. The high-resolution and bias-dependent STM images support the previously suggested atomic structure model composed of six In atoms and three displaced Si adatoms. The STS measurement shows semiconducting surface electronic property with a band gap of 0.8 eV which is consistent with the previous photoemission result. The band gap is properly reproduced by density-functional theory calculations based on the structure model of the magic cluster and is understood as due to the pseudomolecular bonding-antibonding splitting of the In-Si bonds within the cluster. At RT, In adsorbates are found to form well-defined clusters, called initial clusters, which are distinct from the magic clusters. It is found that the initial clusters are composed of the same number of In atoms and metastable to transform into the magic cluster by thermal annealing. This cluster is thus thought to be a precursor state of the magic cluster. The initial clusters have an asymmetric shape, in sharp contrast to the magic cluster, without a rotational symmetry but with a chiral symmetry. The clusters of both chiralities are formed without a preference. The bias-dependent STM images of the initial cluster exhibit not only the similarity but also the difference from the magic cluster. The STS measurement shows the nonmetallic electronic property of the initial cluster with a significantly reduced band gap of 0.4 eV from that of the magic cluster. This largely different electronic property may yield different chemical and physical properties of the clusters formed at different temperature. The detailed atomic structure of the initial cluster remains to be studied. Through the investigation of the detailed atomic structures of the initial clusters and the decayed clusters, one may be able to clarify the atomic scale processes involved in the formation and decay of magic clusters.

ACKNOWLEDGMENTS

This work was supported by MOST through the Center for Atomic Wires and Layers of the CRi program and Yonsei University Research Fund.

*Author to whom correspondence should be addressed; yeom@yonsei.ac.kr

[1] J. J. Lander and J. Morrison, J. Appl. Phys. **36**, 1706 (1965).
[2] J. Nogami, Sang-Il Park, and C. F. Quate, Phys. Rev. B **36**, 6221 (1987).
[3] J. Kraft, M. G. Ramsey, and F. P. Netzer, Phys. Rev. B **55**, 5384 (1997).
[4] S. W. Cho, K. Nakamura, H. Koh, W. H. Choi, C. N. Whang, and H. W. Yeom, Phys. Rev. B **67**, 035414 (2003).
[5] T. Abukawa, M. Sasaki, F. Hisamatsu, T. Goto, T. Kinoshita, A. Kakizaki, and S. Kono, Surf. Sci. **325**, 33 (1995).
[6] J. M. Nicholls, P. Måartensson, G. V. Hansson, and J. E. Northrup, Phys. Rev. B **32**, 1333 (1985).
[7] Eli Rotenberg, H. Koh, K. Rossnagel, H. W. Yeom, J. Schäfer, B. Krenzer, M. P. Rocha, and S. D. Kevan, Phys. Rev. Lett. **91**, 246404 (2003).
[8] S. V. Ryjkov and V. G. Lifshits, e-J. Surf. Sci. Nanotechnol. **1**, 72 (2003).
[9] M. Hupalo and M. C. Tringides, Phys. Rev. B **73**, 041405(R) (2006).
[10] T. Uchihashi, C. Ohbuchi, S. Tsukamoto, and T. Nakayama, Phys. Rev. Lett. **96**, 136104 (2006).
[11] J.-L. Li, J.-F. Jia, X.-J. Liang, X. Liu, J.-Z. Wang, Q.-K. Xue, Z.-Q. Li, J. S. Tse, Z. Zhang, and S. B. Zhang, Phys. Rev. Lett. **88**, 066101 (2002).
[12] J. F. Jia, X. Liu, J. Z. Wang, J. L. Li, X. S. Wang, Q. K. Xue, Z. Q. Li, Z. Zhang, and S. B. Zhang, Phys. Rev. B **66**, 165412 (2002).
[13] M. Y. Lai and Y. L. Wang, Phys. Rev. B **64**, 241404(R) (2001).
[14] J.-F. Jia, J.-Z. Wang, X. Liu, Q.-K. Xue, Z.-Q. Li, Y. Kawazoe, and S. B. Zhang, Appl. Phys. Lett. **80**, 3186 (2002).
[15] V. G. Kotlyar, A. V. Zotov, A. A. Saranin, T. V. Kasyanova, M. A. Cherevik, I. V. Pisarenko, and V. G. Lifshits, Phys. Rev. B **66**, 165401 (2002).
[16] K. Wu, Y. Fujikawa, T. Nagao, Y. Hasegawa, K. S. Nakayama, Q. K. Xue, E. G. Wang, T. Briere, V. Kumar, Y. Kawazoe, S. B. Zhang, and T. Sakurai, Phys. Rev. Lett. **91**, 126101 (2003).
[17] S.-C. Li, J.-F. Jia, R.-F. Dou, Q.-K. Xue, I. G. Batyrev, and S. B. Zhang, Phys. Rev. Lett. **93**, 116103 (2004).
[18] I. Ošt'ádal, P. Kocán, P. Sobotík, and J. Pudl, Phys. Rev. Lett. **95**, 146101 (2005).
[19] Y. L. Wang, A. A. Saranin, A. V. Zotov, M. Y. Lai, and H. H. Chang, Int. Rev. Phys. Chem. **27**, 317 (2008), and references therein.
[20] J. H. Byun, J. R. Ahn, W. H. Choi, P. G. Kang, and H. W. Yeom, Phys. Rev. B **78**, 205314 (2008).
[21] H. Narita, A. Kimura, M. Taniguchi, M. Nakatake, T. Xie, S. Qiao, H. Namatame, S. Yang, L. Zhang, and E. G. Wang, Phys. Rev. B **78**, 115309 (2008).
[22] L. Zhang, S. B. Zhang, Q. K. Xue, J. F. Jia, and E. G. Wang, Phys. Rev. B **72**, 033315 (2005).
[23] G. Kresse and J. Hafner, Phys. Rev. B **47**, 558 (1993); G. Kresse and J. Furthmüller, *ibid.* **54**, 11169 (1996).
[24] D. Vanderbilt, Phys. Rev. B **41**, 7892 (1990).
[25] J. P. Perdew and Y. Wang, Phys. Rev. B **45**, 13244 (1992).
[26] R. Wolkow and Ph. Avouris, Phys. Rev. Lett. **60**, 1049 (1988).
[27] J. Mysliveček, A. Stróżecka, J. Steffl, P. Sobotík, I. Ošt'ádal, and B. Voigtländer, Phys. Rev. B **73**, 161302(R) (2006).
[28] X. F. Lin, H. A. Mai, I. Chizhov, and R. F. Willis, J. Vac. Sci. Technol. B **14**, 995 (1996).